

Unexpected High Winds in Northern New Jersey: A Downslope Windstorm in Modest Topography

STEVEN G. DECKER

Department of Environmental Sciences, Rutgers, The State University of New Jersey, New Brunswick, New Jersey

DAVID A. ROBINSON

Department of Geography, Rutgers, The State University of New Jersey, Piscataway, New Jersey

(Manuscript received 21 November 2010, in final form 26 April 2011)

ABSTRACT

This study presents the first evidence for the occurrence of a downslope windstorm in New Jersey. During the early morning hours of 4 January 2009, an unanticipated strong wind event was observed. Despite a zone forecast calling for winds less than 4 m s^{-1} issued 4 h prior to the event, winds up to 23 m s^{-1} were reported at High Point, New Jersey (elevation 550 m), with gusts to 30 m s^{-1} in its immediate lee (elevation 311 m). These winds were highly localized; a nearby Automated Surface Observing System (ASOS) station (Sussex, New Jersey, 12 km distant) reported calm winds between 0700 and 1000 UTC, just as the winds were peaking near High Point. High Point is the highest point in New Jersey, and is part of the quasi-two-dimensional Kittatinny Mountain extending from Pennsylvania into New York. This study tests the hypothesis that the topography of High Point, upon interacting with the local atmospheric stability and wind profiles, was sufficient to produce a downslope windstorm, thus causing these unusual winds. The results indicate that the presence of a sharp low-level temperature inversion in combination with a northwesterly low-level jet perpendicular to the ridge provided the key ingredients for the strong winds. Linear theory does not appear to explain the winds. Instead, prior studies incorporating nonlinearity predict a trapped lee wave or possibly a hydraulic jump, and model simulations suggest that High Point was indeed tall enough to generate such a wave along with rotors, although observations were not available to confirm this. Given sufficient model resolution, many aspects of this event were predictable. Similar windstorms have occurred before at High Point, but observations show that this event was the most amplified in recent years.

1. Introduction

Downslope windstorms have been well documented in many parts of the world, such as near the Front Range in Colorado [both to its east (Klemp and Lilly 1975) and to its west (Meyers et al. 2003)], west of the Cascade Range (Colle and Mass 1998a,b), along the eastern Adriatic coast (Grisogono and Belusic 2009), and within Greece (Koletsis et al. 2009). While these previous examples involve substantial topographic features, other windstorms have been associated with relatively modest topography. Examples of these less extreme events include those associated with the Falkland Islands (Vosper 2004;

Sheridan and Vosper 2006), and, in the eastern United States, the Great Smoky Mountains (Gaffin 2002, 2009) and the central Appalachians (Manuel and Keighton 2010). Aside from Mount Washington's well-known winds (Hildebrandt and Balling 1998; Martner et al. 2002), topographic influences on airflow in the Northeast have been discussed not in terms of downslope windstorms but rather with regard to their effects on such phenomena as rain shadows (Brady and Waldstreicher 2001) and tornadogenesis (Bosart et al. 2006). Therefore, it was quite unexpected to forecasters and climatologists alike when the New Jersey Weather and Climate Network (Robinson 2005) observed a localized high wind event near High Point, New Jersey, on 4 January 2009.

This study uses theory, observations, and modeling to show that the high-wind event near High Point was a consequence of the interaction between the peculiar geography of High Point and the atmospheric wind and

Corresponding author address: Steven G. Decker, Dept. of Environmental Sciences, Rutgers, The State University of New Jersey, 14 College Farm Rd., New Brunswick, NJ 08901.
E-mail: decker@envsci.rutgers.edu

stability profiles present in the region, namely, a downslope windstorm. Section 2 discusses the geography of the area and provides a synoptic overview of the windstorm based on observations and short-term model forecasts. Section 3 uses mountain wave theory to demonstrate that the atmospheric conditions during the windstorm were consistent with those necessary to produce enhanced winds. Section 4 describes a model simulation of the windstorm, while section 5 summarizes the results.

2. Synoptic overview

a. High Point geography

With an elevation of 550 m, High Point is the highest point in New Jersey. It is not an isolated mountain, but rather part of a quasi-two-dimensional¹ ridge extending from Pennsylvania into New York. This ridge, which has an average elevation of 400 m (see Fig. 1), is known as Blue Mountain in Pennsylvania, Kittatinny Mountain in New Jersey, and the Shawangunk Mountains in New York. To the west and north of this ridge lay the Pocono Mountains of Pennsylvania and Catskill Mountains of New York (Fig. 1). Although Bosart et al. (2006) have suggested that the topography associated with the Catskills has influenced tornadic circulations, we are unaware of any studies showing that the more modest Blue–Kittatinny–Shawangunk ridge can influence wind speeds in relatively quiescent conditions as in this event.

Three stations contained within the New Jersey Weather and Climate Network are located near High Point. The High Point Monument station (HPM) is located near the summit. The High Point station (HPT) is located to the south at the High Point State Park ranger station. (To avoid confusion, High Point in this paper always refers to the topographical feature, whereas HPT refers to observations from the High Point station.) To the east is the Wantage station (WNT). Farther to the south of High Point lies the Automated Surface Observing System (ASOS) station at Sussex Airport in Sussex, New Jersey (FWN; see Fig. 1b). Table 1 gives the elevation of each of these stations and their distance from High Point. All stations have anemometers at the standard height of 10 m except HPM at 7.5 m.

b. The windstorm forecast

The windstorm occurred in northwesterly flow to the southwest of a deep, well-occluded cyclone positioned

over the Canadian Maritimes (Fig. 2). The 0000 UTC 4 January 2009 North American Mesoscale Model (NAM) forecast valid at 0900 UTC later that night showed winds of 15 m s^{-1} at 850 hPa over New Jersey (Fig. 2a). Noted warming was forecast from New Jersey up to Maine, with a thermal ridge in the 0°C isotherm present over that region. This is suggestive of adiabatic warming that would occur as air parcels descend in the lee of the Appalachian Mountains, a pattern characteristic of a föehn wind. The topographically induced subsidence suggested by the 850-hPa isotherms was forecast to be enhanced by synoptic-scale forcing for descent, as the region was located upstream from the primary trough axis off the coast (Figs. 2b and 2c). However, within this larger-scale subsidence, the NAM forecast contained small regions of 700-hPa ascent generally parallel to the Appalachians in Maine, northeastern New York, and eastern Pennsylvania. Ascent at this level just downstream of mountain ridges is consistent with the presence of mountain waves (e.g., Durran and Klemp 1983, their Fig. 4). The NAM also forecast winds at upper levels (Figs. 2c and 2d) to be from the northwest, implying unidirectional shear over the region.

Although the NAM forecast contained hints that topography would perturb the flow across the Northeast, these perturbations were not expected to affect the surface. Accordingly, the National Weather Service (NWS) zone forecast for Sussex County (the northernmost part of New Jersey) was routine:

SUSSEX NJ-
845 p.m. EST SAT JAN 3 2009
.OVERNIGHT...MOSTLY CLEAR. LOWS
AROUND 15. NORTHWEST WINDS 5 TO 10
MPH.

c. Observations of the windstorm

The 0900 UTC 4 January 2009 observations from the standard surface network, valid about 7 h after that forecast was issued, show that the forecast appeared to be on track (Fig. 3). Indeed, observations from FWN indicated clear skies, calm winds, and temperatures approaching the forecasted lows. However, a closer examination reveals another story. Despite the calm winds at FWN, HPM reported winds of 20.5 m s^{-1} (40 kt) at 0945 UTC, and WNT experienced wind gusts of 24 m s^{-1} (46 kt) at 0800 and 1000 UTC. These winds were nearly double what other stations in the area experienced. For instance, Mount Pocono, Pennsylvania (MPO), reported a gust to 12 m s^{-1} (24 kt) at 0500 UTC, the highest winds in the standard network near High Point. Farther to the northeast (and closer to the cyclone), other notable gusts were measured, including 12 m s^{-1} (23 kt) at Montgomery, New York

¹ By *quasi-two-dimensional*, we mean that the terrain height changes much more rapidly in the cross-ridge direction than in the along-ridge direction.

(MGJ), at 0700 UTC; 14 m s^{-1} (27 kt) at Albany, New York (ALB), at 0300 UTC; and 16 m s^{-1} (32 kt) at North Adams, Massachusetts (AQW), at 0200 UTC.

The Mesowest network of mesonets (Horel et al. 2002) provided additional observations outside the standard network, including wind gusts as strong as 13 m s^{-1} (25 kt) at Willow, New York, in the Catskills and 18 m s^{-1} (35 kt) at Peru, Massachusetts, in the Berkshires. Table 2 compiles the windiest Mesowest observations from the region. However, even with this additional data source, no known observations exist of winds approaching those measured near High Point.

Figure 4 shows the evolution of the winds throughout the event as observed at the four stations closest to High Point. One station (FWN) is an ASOS station that reports sustained winds and wind gusts according to standard conventions. Two stations (WNT and HPT) reported sustained winds (a 5-min average) and wind gusts every hour, but the wind gust that is reported corresponds to the highest wind speed observed only over the previous 5 min, not over the previous hour. Finally, HPM reported the instantaneous wind every 15 min. The measurements at HPM are therefore somewhere between what the wind speed and wind gusts would have been had the same data logging been used at HPM as was used at the other stations. The advantage of the instantaneous wind is that it shows the gustiness of the winds during the event, with fluctuations of almost 10 m s^{-1} in the wind speed over a 15-min period. Since downslope windstorms are well known to contain extremely gusty winds (Klemp and Lilly 1975), this provides evidence that the topography was playing some role in perturbing the large-scale flow near High Point. It is important to note that, although the hourly observations from WNT indicate a peak wind of 24 m s^{-1} (46 kt), the daily peak wind is stored, and that value was found to be 30 m s^{-1} (58 kt).

The observations show that winds at WNT, HPM, and FWN were similar early in the evening (Fig. 4). It is not until 0600 UTC that winds close to High Point diverge from the winds at FWN, although notable wind fluctuations as early as 0200 UTC at WNT suggest that mountain waves may have been establishing themselves by then. (The model results discussed later will agree on this point.) For the rest of the overnight period, FWN reported calm winds as HPM and WNT winds strengthened. Nocturnal boundary layer decoupling in the valley location of FWN cannot explain the disparity in the wind field between these stations because the wind differences remained well past sunrise to about 1600 UTC.

The winds at the ranger station (HPT) are much weaker than the other High Point stations, and even weaker than FWN except during the early morning hours. These weak winds are likely due to the sheltered location of that

station, which makes the wind gusts at HPT roughly approximate to the wind speeds at well-sited WNT for much of the night. It is for this reason that we compare wind gusts from generally sheltered Mesowest stations (Table 2) to forecast wind speeds in section 4.

Previous work has demonstrated that mountain waves can be extremely sensitive to the wind and stability profiles upstream of the topographic forcing (Reinecke and Durran 2009a). Unfortunately, High Point is rather remote from upper-air observation locations, making it difficult to determine with confidence the atmospheric profile there. Nonetheless, an examination of nearby soundings can provide some sense of the conditions at High Point. Nearby stations include Buffalo, New York (BUF), 382 km west-northwest (upstream); ALB, 174 km north-northeast; and Upton, NY (OKX), 158 km east-southeast (downstream). Figure 5 displays the soundings from these locations taken at 1200 UTC 4 January 2009.

In line with many idealized studies of mountain waves and downslope windstorms, the atmosphere consists of four layers based on these soundings (three in the case of BUF). Layer 1, closest to the surface, is a nearly isentropic layer found in the ALB and OKX soundings. This layer was also present at High Point, as temperature observations from HPM, HPT, and WNT (not shown), after accounting for elevation differences, indicate that a dry-adiabatic lapse rate was present near the ground. Layer 2 extends to about 800 hPa, is very stable, and approximates a discontinuity in the potential temperature field. Layer 3 covers the rest of the troposphere and consists of a relatively uniform lapse rate close to moist neutrality. Finally, the stratosphere constitutes the fourth layer. Although there is no critical level in these soundings (except BUF), the presence of a low-level jet within the inversion (again, except BUF) implies that the shear vector reverses direction, which has been proposed to act like a critical level (Durran 1986). The layered structure to the potential temperature field is also favorable for mountain wave activity (Klemp and Lilly 1975).

However, the distance from these soundings to High Point calls into question their representativeness. Thompson et al. (2003) found that soundings based on the Rapid Update Cycle (RUC) were reasonably accurate when compared to observations. Therefore, the 0900 UTC 4 January 2009 cycle of the RUC was obtained on a 20-km grid to generate a plausible sounding just upstream from High Point (Fig. 5d). This sounding is similar to the OKX and ALB soundings. The same four layers are present, as is the low-level jet within the stable layer.

Although Thompson et al. (2003) found reasonable agreement between their RUC and observed soundings, in this case the agreement is less spectacular. A comparison

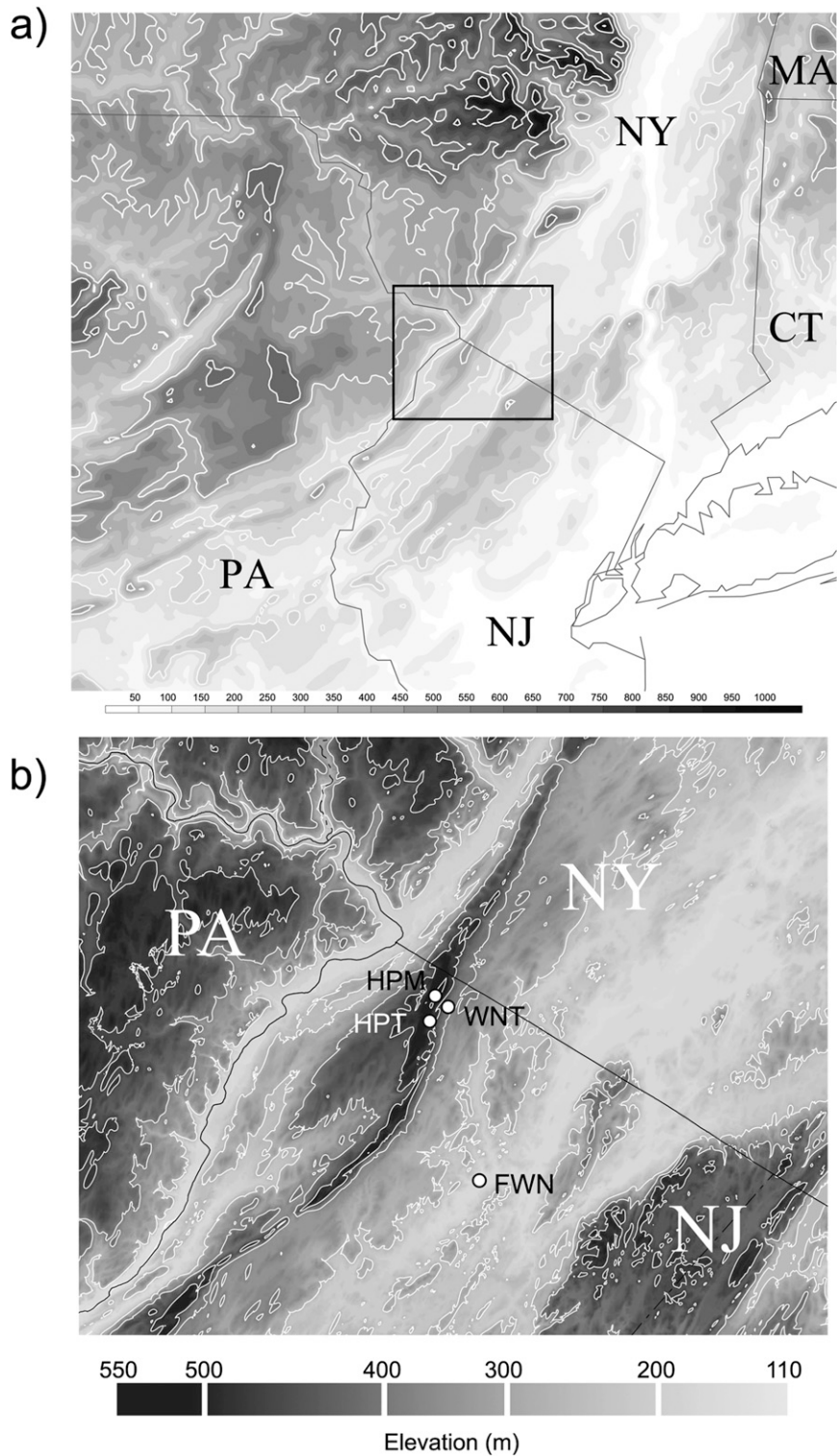


FIG. 1. (a) Regional depiction of terrain height (contoured every 200 m, shaded according to legend) in northern NJ, eastern PA, southern NY, and western CT and MA. The rectangle delineates the area shown in the bottom panel. (b) High-resolution topography near High Point (contoured every 100 m, shaded according to legend). Four surface stations in the area are labeled as described in the text. State (county) borders are solid (dashed).

between the 3-h forecast from this cycle and the concomitant soundings indicates that average absolute temperature errors exceed 1°C below 500 hPa (Fig. 5). In general, the RUC soundings are too warm near the surface and too cold at inversion top, thus weakening the severity of the inversion. [To be fair, Thompson et al. (2003) compared 0- and 1-h forecasts to observations.] Interestingly, the 0900 UTC High Point sounding from the RUC more closely matches the 1200 UTC OKX observations than does the 3-h RUC forecast at OKX. This implies the RUC sounding at High Point may be more reasonable than the comparison of the 3-h forecast would suggest. Furthermore, the 1200 UTC RUC analyses are in much better agreement with the observations. Therefore, we use the RUC sounding analyzed near High Point as if it were an observation.

Assuming the RUC sounding is representative of the conditions near High Point, the base of the temperature inversion was very close to the summit. The low-level jet of 17 m s^{-1} (32 kt) in the sounding had its core about 220 m above the summit, but the observed wind gusts discussed previously were up to 13 m s^{-1} (26 kt) stronger than this jet maximum. This disparity suggests that the local topography significantly amplified the winds near High Point, by as much as 75% if the RUC sounding is accurate.

3. Mountain wave theory

What mechanisms might be responsible for the observed amplification of the winds near High Point? From the observations, it seems clear that the enhanced downslope winds reported at Wantage are the result of mountain wave activity. The question then becomes one of determining the mechanisms responsible for generating a strong mountain wave response.

Previous studies have proposed a number of different mechanisms to explain the occurrence of flow amplification downstream of mountain ridges. Klemp and Lilly (1975) used linearized equations and an analytic approach to show that downslope windstorms can occur from the reflection of vertical gravity waves excited by the topography. These gravity waves can be reflected off a low-level inversion located a certain distance above the mountaintop, or off the tropopause, or both. Clark and Peltier (1984) suggested that a critical level (the level at which the cross-barrier component of the flow goes to zero) could provide another gravity wave reflection mechanism. Even if a critical level is not present, breaking mountain waves may trap gravity wave energy beneath a self-induced critical layer. Many subsequent studies (e.g., Durran 1986; Colle and Mass 1998a; Gaffin 2009) have shown that, while not necessary for downslope windstorm development, the presence of a critical level or

TABLE 1. Elevation of various surface stations capturing the high-wind event of 4 Jan 2009 and their distances from the summit of High Point.

Station	Elev (m)	Distance from High Point summit (km)
HPM	535	0.1
HPT	422	1.6
WNT	310	1.2
FWN	128	12

wave breaking increases the likelihood and strength of windstorms. Colle and Mass (1998b) related reverse shear (where not the wind, but the wind shear perpendicular to the ridge goes to zero) to subsequent wave breaking.

Durran (1986) argued that nonlinear interactions are important for the generation of downslope windstorms. In contrast to Klemp and Lilly's (1975) linear theory, where even an infinitesimally small mountain would generate a response, Durran (1986), by analogy to hydraulic theory, stressed that nonlinearities would result in the existence of a critical threshold in the Froude number above which a transition from subcritical to supercritical flow would occur. The result of such a transition is a downslope windstorm.

Vosper (2004) used numerical experiments of flow over an isolated 2D mountain in the presence of a strong low-level inversion to examine how the strength and position of a low-level inversion in relation to the characteristics of the mountain affected the resulting flow patterns. He found that weak inversions prevented any low-level reflection of the vertically propagating gravity waves. Stronger inversions resulted in trapped lee waves, trapped lee waves with rotors, or, in the most severe cases, hydraulic jumps. Vosper's (2004) results were further extended by Sheridan and Vosper (2006) to show that the width of the mountain had little effect on the flow evolution.

Results from the idealized and numerical experiments described above were applied to the atmospheric and topographic conditions observed at High Point. First, the linear theory of Klemp and Lilly (1975) for the case of a neutral layer beneath a sharp inversion was applied to the RUC-based conditions at High Point. According to these calculations (not shown), the strongest surface wind perturbation expected at High Point would be 7.3 m s^{-1} , which is much less than the observed amplification of 13 m s^{-1} . Therefore, it appears that the linear theory is not enough to explain the windstorm; nonlinear effects may have been equally important.

Durran (1986) presents one approach that includes nonlinearity. Here, conditions analogous to a hydraulic jump are indicative of a downslope windstorm. Two

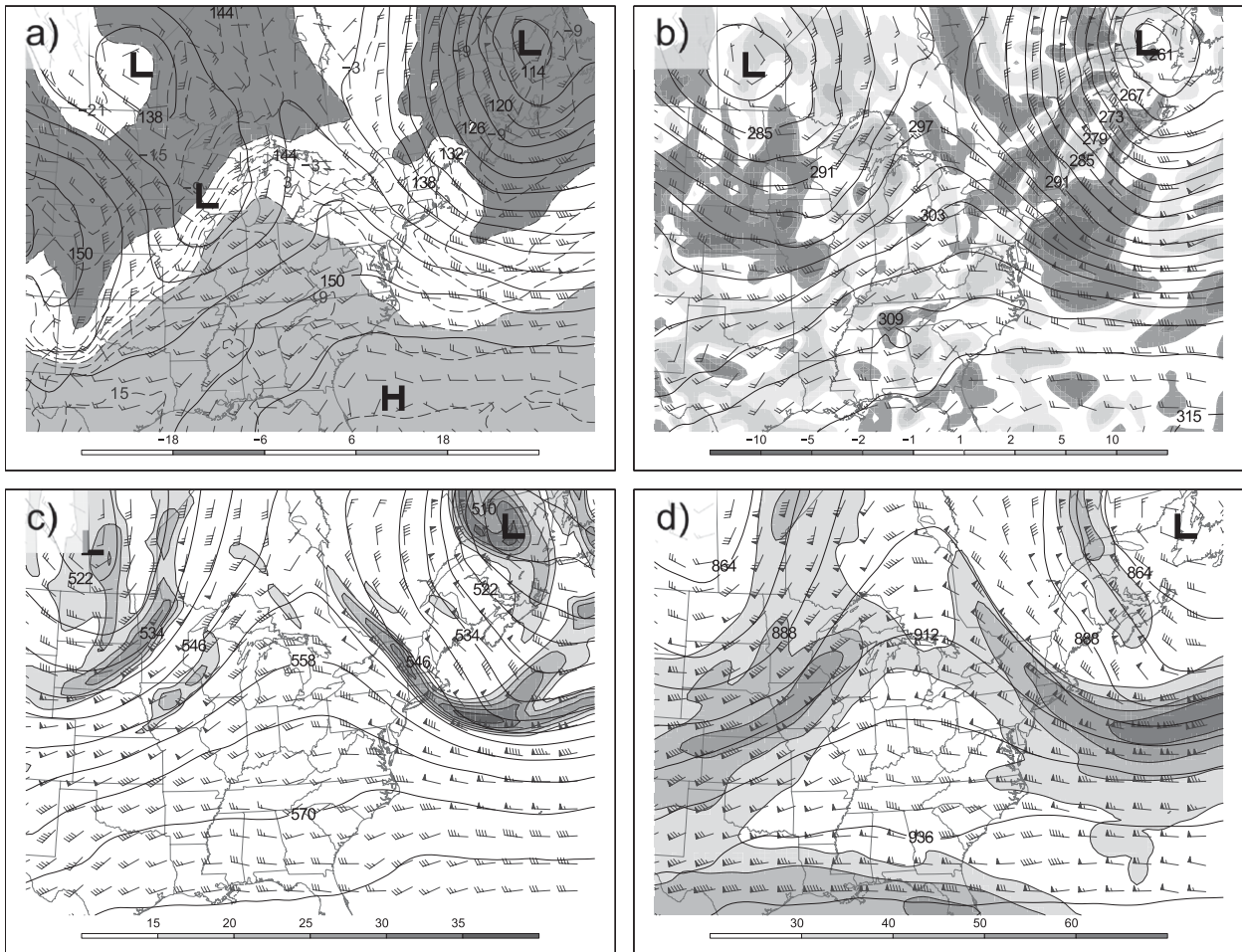


FIG. 2. Upper-level conditions at 0900 UTC 4 Jan 2009 based on a 9-h forecast of the NAM on the National Centers for Environmental Prediction's 40-km Grid 212: (a) 850-hPa winds (barbs, standard convention), temperature (dashed, every 3°C , and shaded according to scale), and geopotential height (solid, every 3 dam); (b) 700-hPa winds, vertical motion ($-\mu\text{b s}^{-1}$, shaded according to scale), and geopotential height (solid, every 3 dam); (c) 500-hPa winds, absolute vorticity ($\times 10^{-5} \text{ s}^{-1}$, shaded according to scale), and geopotential height (solid, every 6 dam); and (d) 300-hPa winds, wind speed (m s^{-1} , shaded according to scale), and geopotential height (solid, every 12 dam).

aspects of the observed sounding are favorable for downslope windstorms according to this theory. First, the Brunt-Väisälä frequency in the low-level inversion (0.029 s^{-1}) was greater than the Brunt-Väisälä frequency in the lower stratosphere (0.022 s^{-1}). Second, the Froude number was found to change from subcritical to supercritical if the depth of the fluid is set to extend from the surface to any isobaric level between 889 and 901 hPa. Figure 5 indicates that these levels were within the inversion layer and thus plausible estimates for the depth of the lowest atmospheric layer.

The results of Vosper (2004), which are encapsulated in the regime diagram reproduced in Fig. 6, provide another approach that would account for nonlinearity. This regime diagram is particularly useful because it was constructed based on the occurrence of downslope windstorms in the

Falkland Islands downstream of mountains not much higher than High Point in the presence of a sharp low-level inversion. In other words, the conditions used in these numerical experiments are quite close to the High Point windstorm observations. A number of parameters relevant to the atmospheric flow near High Point are collected in Table 3 to facilitate a comparison between the observations discussed previously and the Vosper (2004) experiments. The results show that High Point fell within the part of the regime diagram associated with either trapped lee waves and rotors or a hydraulic jump, as indicated by the star in Fig. 6. Both of these cases are associated with significant nonlinear amplification of the near-surface winds. This provides additional evidence that previous theories related to downslope windstorms explain the high winds observed near High Point.

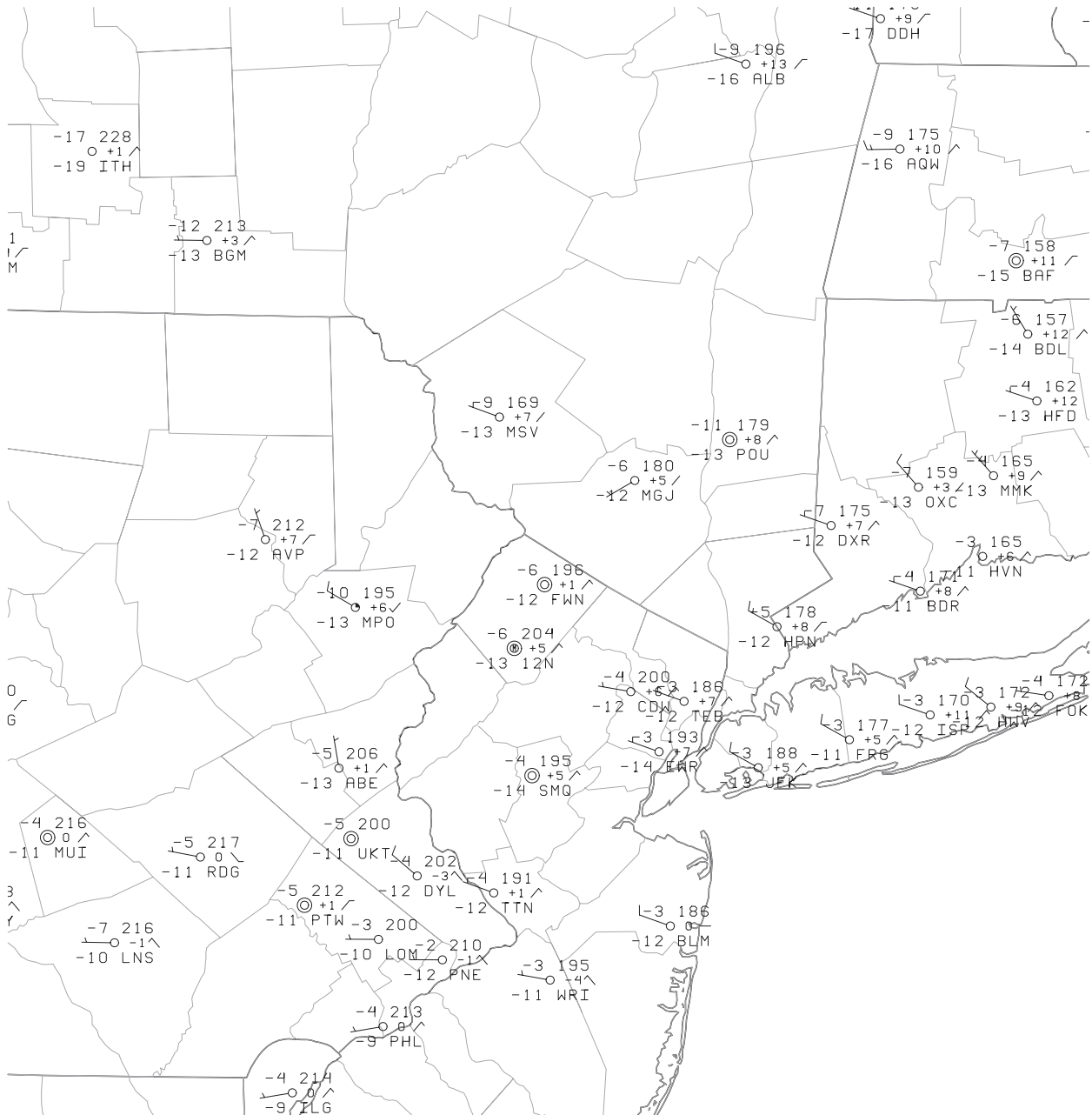


FIG. 3. Surface observations at 0900 UTC 4 Jan 2009 using standard convention. Temperatures are in °C.

In summary, the observations of the wind near High Point match previous research into downslope windstorms in the following ways:

- 1) Gustiness of the winds was observed (Klemp and Lilly 1975).
- 2) The strongest winds were present to the lee of the mountaintop (Klemp and Lilly 1975).
- 3) The leeward slope near High Point is steeper than the windward slope (Miller and Durran 1991), as seen by the smaller spacing between the 400- and 500-m contours in the lee in Fig. 1b.
- 4) The two-dimensional nature of Kittatinny Mountain makes the flow pattern similar to that seen in idealized studies, although Epifanio and Durran (2001) have shown that three-dimensional effects can be important even for long quasi-2D ridges.
- 5) Winds at mountaintop level were significant and oriented perpendicular to the ridge (Colle and Mass 1998b).

TABLE 2. The 12 windiest stations in the Mesowest network within the region of the windstorm based on the maximum wind gusts observed at each station during the High Point windstorm.

Station	Elev (m)	Forest* (%)	Max gust (m s^{-1})
Peru, MA	577	84	17.8
New Hartford, CT	323	82	13.9
Willow, NY	327	39	13.4
Cooperstown, NY	594	44	11.2
Barkhamsted, CT	293	61	10.3
Pine Bush, NY	139	68	10.3
Belleayre Mountain, NY	594	76	9.8
Thomaston, CT	275	67	9.4
U.S. Military Academy (USMA), West Point, NY	281	68	9.4
Southington 2, CT	59	5	8.9
Thornhurst, PA	566	61	8.9
Avon, CT	129	51	8.5

* Forest is the percentage of land within 500 m of the station covered by forest according to Mesowest metadata.

- 6) A strong inversion was present just above the mountaintop (Meyers et al. 2003).
- 7) Reverse shear was present (Colle and Mass 1998b).
- 8) Synoptic-scale descent was present (Meyers et al. 2003).
- 9) The Froude number switched from subcritical to supercritical as low-level air passed over the ridge (Durran 1986).
- 10) The combination of the ratio of the height of High Point to the inversion height and the Froude number places High Point in an area of large nonlinear amplification on the Vosper (2004) regime diagram.

Although many ingredients for a significant wind event appear to have been in place, Reinecke and Durran

(2009a) have shown that, even when nonlinear numerical models are used, whether a downslope windstorm forms can be extremely sensitive to the initial conditions used. Often, models overpredict the occurrence of downslope windstorms (Nance and Coleman 2000). Therefore, the presence of all of the favorable ingredients mentioned above is no guarantee that strong winds will occur. Furthermore, should strong winds occur, the details of the windstorm evolution typically require numerical modeling to discern (Koletsis et al. 2009). Finally, idealized numerical modeling often occurs at high resolution, but forecasters have limited access to model output with such resolution. Thus, the grid spacing necessary to capture this windstorm is an important question to address.

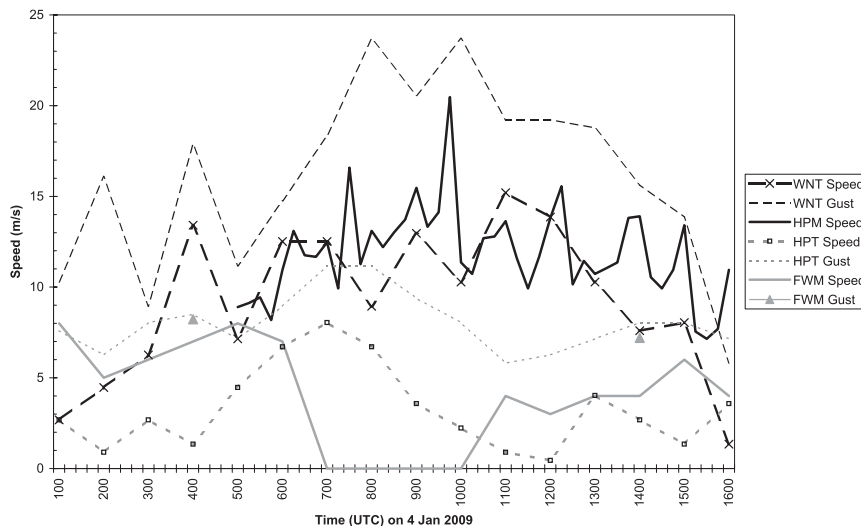


FIG. 4. Wind observations (m s^{-1}) between 0100 and 1600 UTC 4 Jan 2009. Shown are the WNT wind speed (thick, long-dashed line with cross) and gust (thin, medium-dashed line), HPM instantaneous wind speed (thick, solid line), HPT wind speed (thick, short-dashed line with square) and gust (thin, short-dashed line), and FWM wind speed (thick, solid gray line) and gust (triangles).

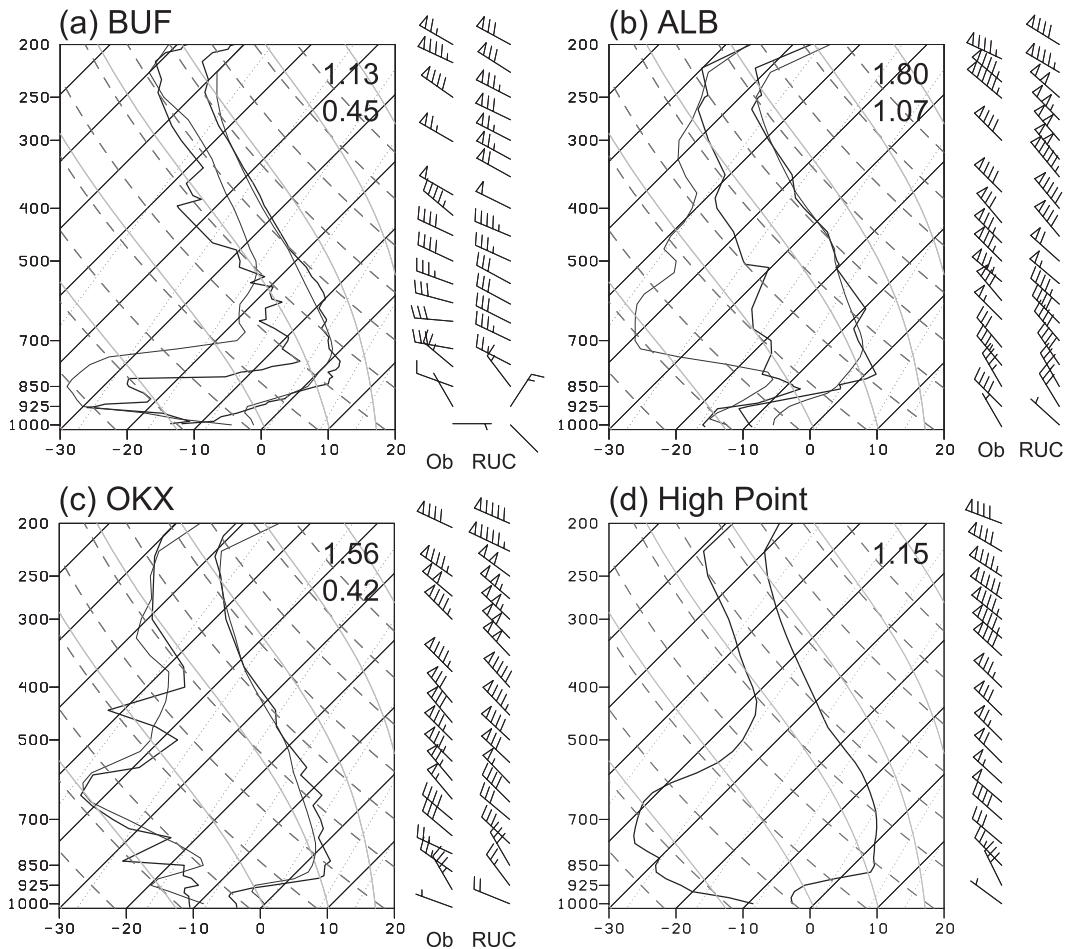


FIG. 5. Skew T -log p diagram of upper-air observations (thick) and corresponding 3-h RUC forecasts (thin) for (a) BUF, (b) ALB, and (c) OKX valid at 1200 UTC 4 Jan 2009. (d) As in (a)–(c), but showing the 0900 UTC 4 Jan 2009 RUC analysis just upstream of High Point where NY, PA, and NJ meet. Values in the upper-right corners in (a)–(c) show the average absolute temperature error below 500 hPa ($^{\circ}\text{C}$) of the (top) 3-h RUC forecast and (bottom) 1200 UTC RUC analysis, and in (d) represent the error when comparing the 0900 UTC RUC analysis to the 1200 UTC OKX sounding.

4. Model simulation

The Weather Research and Forecasting Model (WRF; Skamarock et al. 2008) was used to further examine the role topography played in this event. Five domains were employed, with grid spacings of 36, 12, 4, $\frac{4}{3}$, and $\frac{4}{9}$ km for domains 1–5, respectively. Sixty vertical levels were used on the outer three domains, with an increase to 117 levels on the inner domains. The model was initialized from North American Regional Reanalysis data valid at 0000 UTC 4 January 2009, or 6–12 h before the event. The parameterizations chosen included the Dudhia shortwave scheme (Dudhia 1989), the Rapid Radiative Transfer Model (RRTM) longwave radiation scheme (Mlawer et al. 1997), the Kain–Fritsch cumulus scheme (Kain 2004) on the outer two domains,

and the WRF Single-Moment Three-Class (WSM3) microphysics package (Hong and Lim 2006). Doyle and Durran (2002) have pointed out the importance of surface friction on the evolution of mountain waves, particularly when rotors are involved, as the Vosper (2004) regime diagram suggests may be the case. To that end, the model simulation represents surface friction through the use of the Yonsei University (YSU) boundary layer scheme (Hong et al. 2006), the Monin–Obukhov surface layer scheme (Monin and Obukhov 1954), and the Noah land surface model (Chen and Dudhia 2001). Reinecke and Durran (2009b) showed that low-order advection schemes perform poorly when simulating mountain waves. The fifth-order advection used by the WRF, combined with the fact that High Point is a $50\Delta x$ -wide mountain on domain 5 (or $6\Delta x$ wide for the steepest

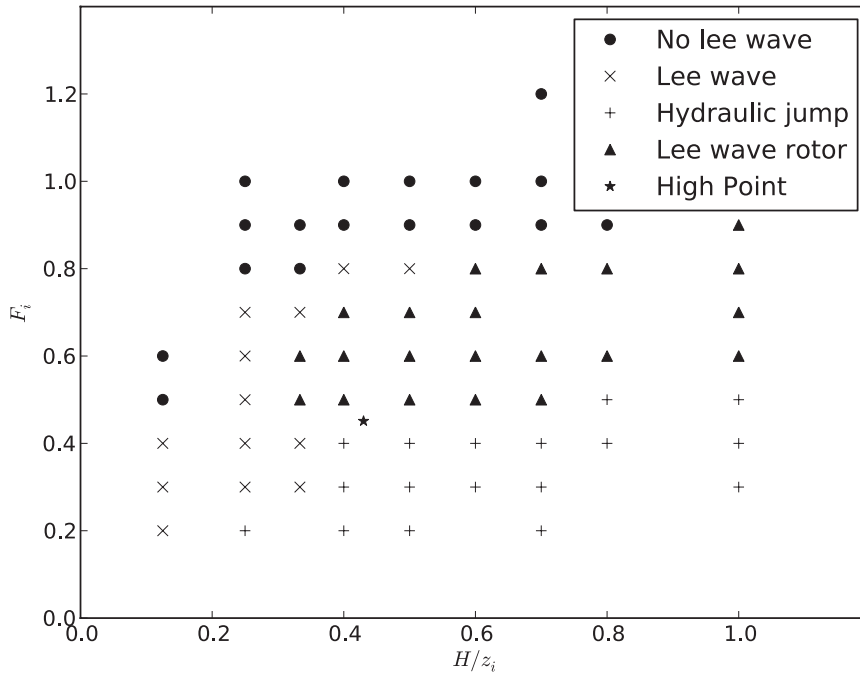


FIG. 6. Regime diagram showing the terrain-induced phenomena that occur for various combinations of the parameters H/z_i and F_i . The parameter combination representative of the conditions near High Point is marked with a star. [Adapted from Vosper (2004).]

portion centered on the peak itself), thus limits these numerical errors.

Figure 7 shows how the reduced grid spacing results in greater accuracy in the terrain depiction on the innermost domains. On domain 2 (Fig. 7a), Kittatinny Mountain does not exist. On domain 3 (Fig. 7b), Kittatinny Mountain appears, but the Highlands to the east are shown at a higher elevation than High Point. Domain 4 (Fig. 7c) is the first domain to capture the key topographic features in their entirety, and domain 5 (Fig. 7d) further sharpens the width of Kittatinny Mountain around High Point. Improving terrain resolution through further reductions in grid spacing would require the use of a higher-resolution terrain dataset than that supplied with the WRF model, but we will see that the current configuration of the model was adequate without such measures.

Figure 8 shows a model sounding taken from the 9-h WRF forecast just upstream from High Point over the Delaware River (where New Jersey, Pennsylvania, and New York meet) superimposed upon the RUC sounding displayed earlier in Fig. 5d. The WRF wind profile is almost identical to the RUC analysis, with the exception of more severely veered winds within the inversion in the RUC. Temperature and dewpoint differences are much more notable below 500 hPa, but these may be the result of differing topographies in the two models. The reasonableness of the WRF sounding temperature is

bolstered by the fact that surface observations indicate that a dry-adiabatic lapse rate was present from the valley floor to High Point, which matches the WRF sounding, not the RUC. Despite this uncertain verification, the model forecast was able to predict key elements of the wind field at both WNT and FWN, which is shown next.

Figure 9 shows the 9-h forecast of the winds at various levels as well as the WRF Post Processor and Verification Systems (WRFPOST) wind gust diagnostic (Chuang et al. 2004) for stations WNT and FWN, with the corresponding observations overlain. Although model solutions at WNT and HPM showed similar structures (thus,

TABLE 3. Values for various parameters relevant to the High Point wind event.

Symbol	Name	Value
\bar{U}	Mean horizontal wind (lowest layer)	11 m s ⁻¹
$\Delta\bar{\theta}$	Inversion strength	17 K
z_i	Inversion height	990 m
H	Mountain height	428 m
$\bar{\theta}_0$	Reference potential temperature	271 K
$g' = g(\Delta\bar{\theta}/\bar{\theta}_0)$	Reduced gravity	0.62 m s ⁻²
$F_i = \bar{U}/\sqrt{g'z_i}$	Froude number	0.45
H/z_i	Mountain height to inversion height ratio	0.43

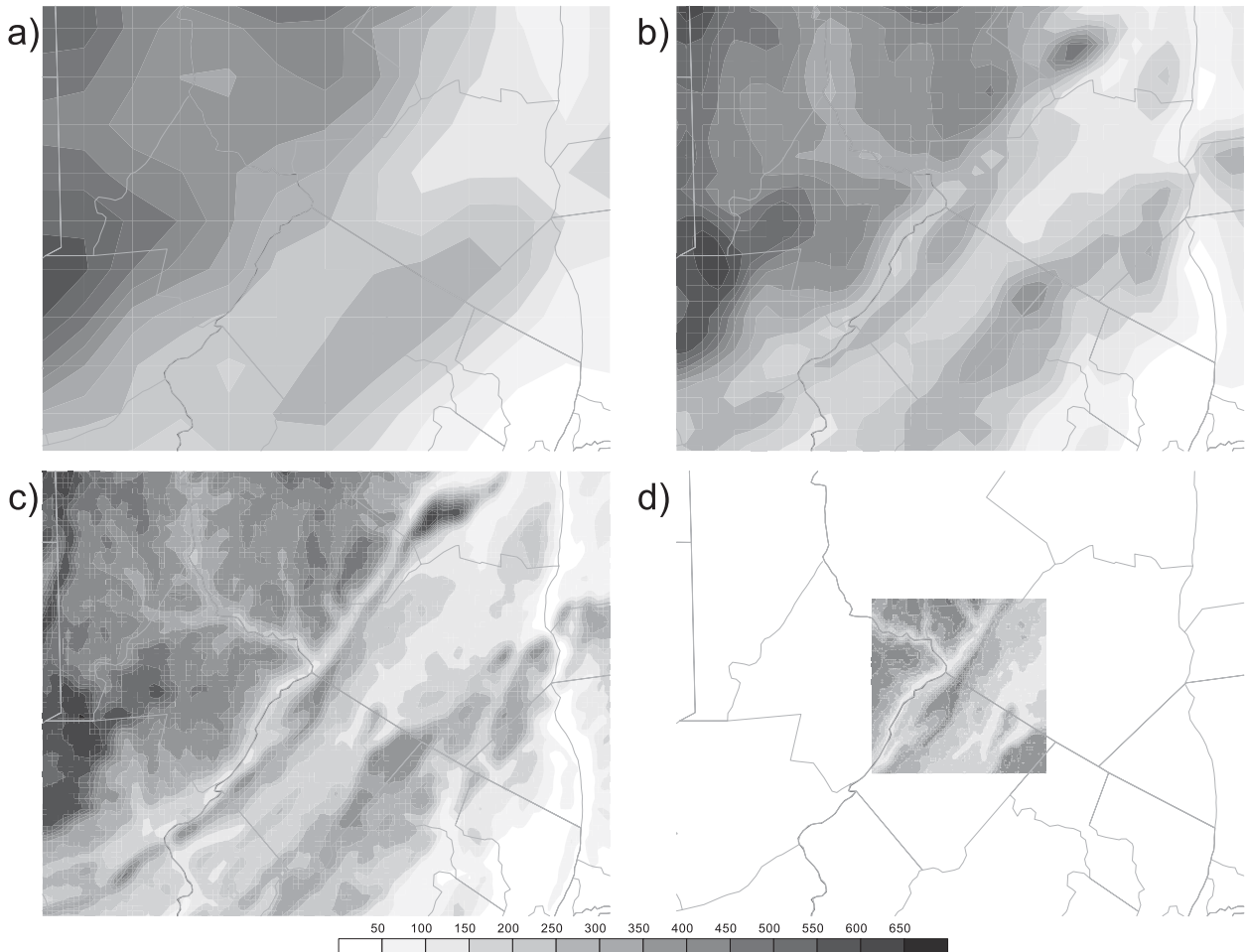


FIG. 7. WRF terrain (m, shaded according to legend) on the innermost domains. Domains (a) 2, (b) 3, (c) 4, and (d) 5 are shown.

only WNT winds are shown), a few important differences between those locations emerged. Peak winds at WNT were up to 2 m s^{-1} stronger than the winds at HPM, so that the model matched the observations in predicting stronger winds in the lee, and the time of maximum wind was a few hours later at WNT (1100 UTC) relative to HPM (0700 UTC). Winds at WNT were generally underforecast, whereas winds at FWN were generally overforecast, yet significant differences in the wind speed between these stations were still captured.

At WNT, the 10-m wind speed was too low, but the wind at the lowest model level matched the observations well (Fig. 9a). The timing of the peak winds at WNT in the model (1100 UTC) matched the observations exactly. The model also reflected the oscillations in the wind that were observed around 0400 UTC (although in opposite phase) and correctly shut down the windstorm at 1600 UTC. The wind gust diagnostic was also too weak, and winds even four model layers above the surface were not able to capture the force of the observed gusts.

At FWN, the 10-m winds generally captured the observed winds well (Fig. 9b). Although the model simulation underestimates the duration of the calm winds, it does at least partially capture the lull. The wind gust diagnostic, on the other hand, vastly overpredicted the observations, which were devoid of gusts except at 0400 and 1400 UTC (Fig. 4). To summarize, the model forecasted strong winds at WNT, and accurately localized those strong winds to the immediate vicinity of High Point, but did not capture the full extent of the amplification, even on domain 5.

The much larger domain 4 best depicts the spatial variability of the wind forecast across the region (Fig. 10). The forecast, even on domain 4, showed that the strongest winds in New Jersey would indeed be near High Point, but other regions of strong winds are present as well, particularly over the Catskills to the north and in the lee of the Taconic Range to the northeast. Lee waves are abundant, although they appear to dissipate just before reaching the New York City metropolitan region.

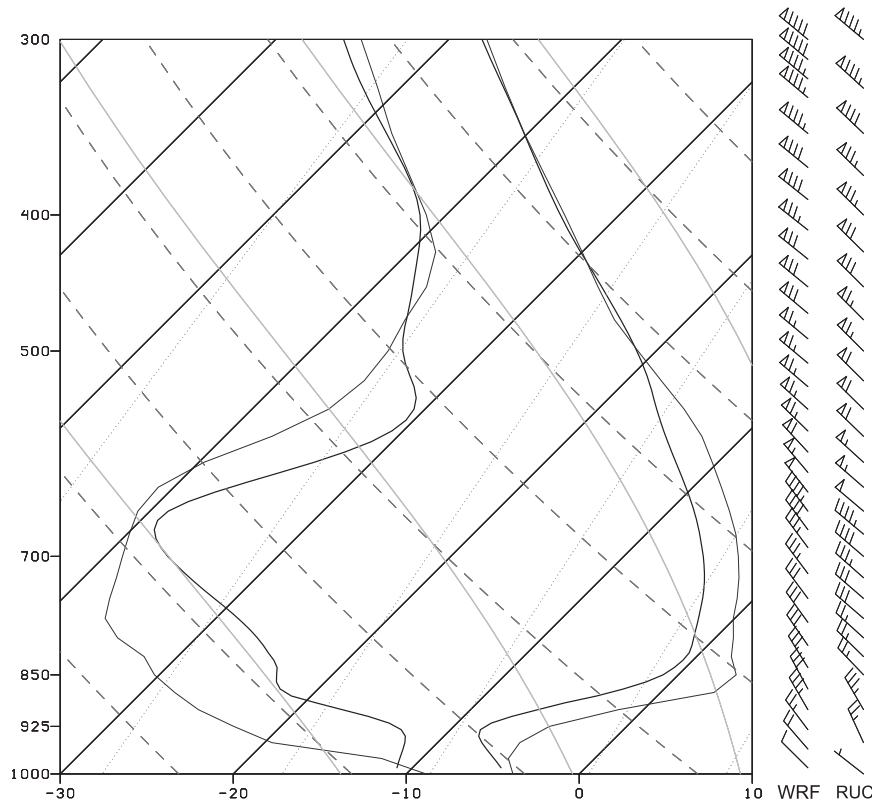


FIG. 8. Skew T -log p diagram of upper-air conditions on domain 5 just upstream of High Point. The profiles are taken from the 9-h WRF forecast (thick) and RUC analysis (thin) valid at 0900 UTC 4 Jan 2009.

The widespread nature of the lee waves is consistent with the strong inversion present across the region. The strong winds over the Catskills correspond to high elevations where the mountaintops reach the height of the low-level jet. The fact that the Catskills extend above the inversion layer is also reflected by the presence of a wake downstream across the Hudson Valley (a wake from the Adirondacks is present at the top of Fig. 10 as well). Thus, those strong winds are not as exceptional as they may seem at first. However, the more modest topography of western Connecticut (recall Fig. 1a) generates significant wind gusts within lee waves as well. A cross section in this area (not shown) reveals that a higher inversion in conjunction with stronger low-level winds (consistent with the Albany sounding) and modest mountain wave activity allows the WRFPOST gust diagnostic to identify the low-level jet as a source of potential wind gusts. The strong wind gusts forecast farther north are less surprising given the increased terrain heights in that region. However, comparisons with observations show that, in many areas, the WRFPOST gust diagnostic greatly overestimates reality, as was seen in the verification at FWN. Therefore, a better way to

examine the performance of the WRF forecast winds is through a comparison of the 10-m winds, which were close to the observations at both FWN and WNT.

Figure 11 shows the model forecast of the 10-m sustained wind field, overlain with surface observations, including WNT and data acquired through Mesowest. Based on our experience with HPT, we assume that on balance Mesowest stations are sheltered from the wind (recall Table 2) such that their wind gust observations approximate what their wind speed measurements would have been had they been located outside of forested regions. These wind gusts are shown in smaller type in Fig. 11. In this depiction, the strong winds near High Point stand out more clearly, and most observations correspond with the forecast reasonably well.

Indeed, the winds at High Point are forecast to be the strongest winds in the state at this time. The nearest areas to have higher winds forecasted are individual grid boxes in the Poconos (A), farther north along the ridge in New York (B), and in the Taconic Range of western Connecticut (C). Regions where stronger winds are forecast over larger areas include the higher terrain of the Catskills (D) and Berkshires (E). Mesowest observations of wind

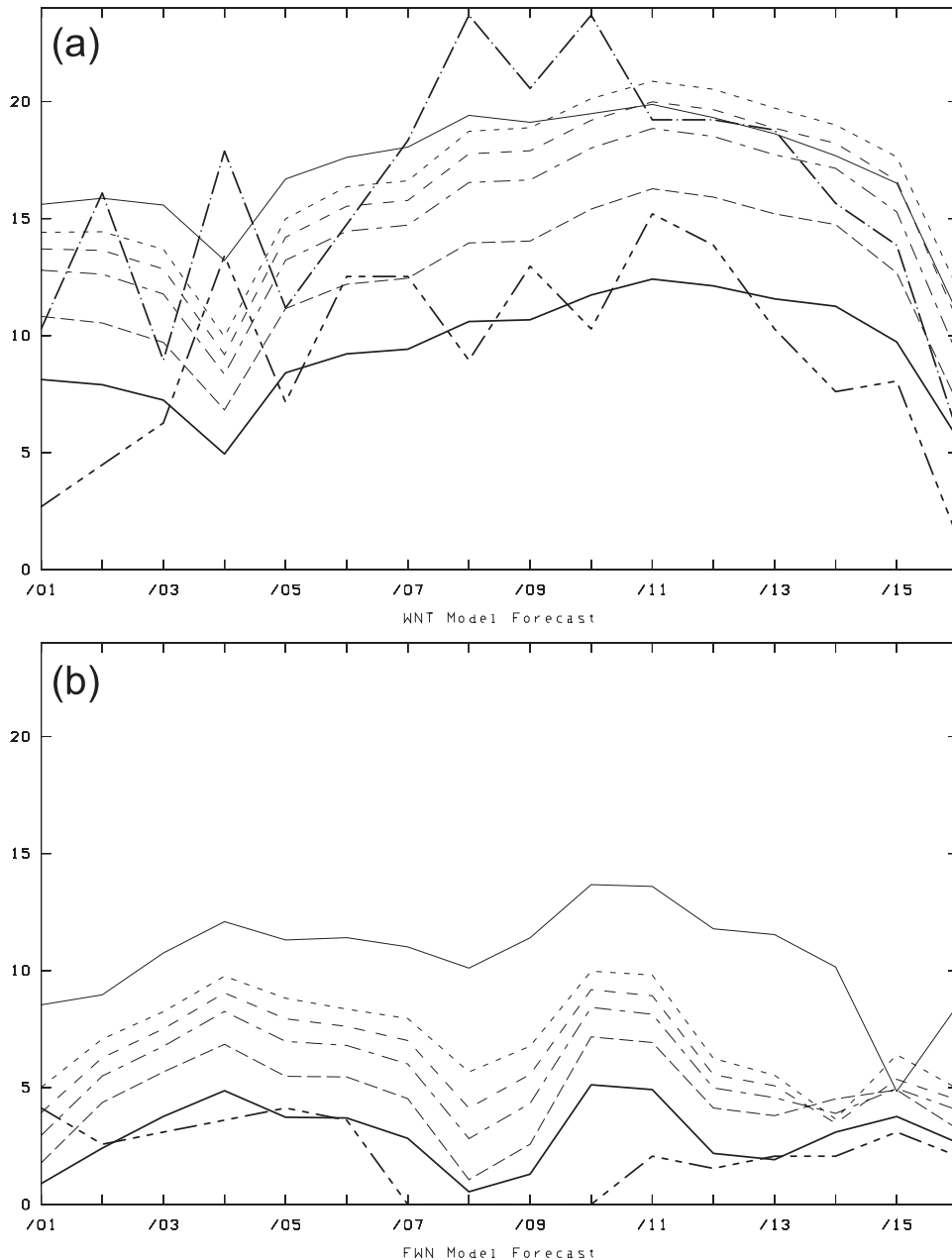


FIG. 9. Time series of winds (m s^{-1}) at (a) WNT and (b) FWN on domain 5 from the WRF forecast initialized at 0000 UTC 4 Jan 2009. The data include the 10-m wind (thick solid line), 10-m wind gusts (thin solid line), and the four lowest model levels (dash length shortens with height). The corresponding observed winds (thick dashed line) and gusts (thick dashed-dotted line, for WNT only) are also shown.

gusts closely match the forecast wind speeds in these regions, but no observations exist at the numerous small-scale wind maxima generated in the WRF forecast. Therefore, the isolated nature of the windstorm at High Point is confirmed, but the possibility exists that equally strong winds could have existed outside New Jersey that went unobserved. The fact that the strongest winds were

isolated even in the model simulation supports the notion that topographic amplification was sensitive to a particular combination of terrain and inversion heights that were only present in some parts of the domain.

A few areas with large disparities between the observed and simulated winds exist, but these disparities can be explained. For example, Cooperstown, New York (F), and



FIG. 10. The 9-h forecast of 10-m wind speed (m s^{-1} , according to reference vector, $<2 \text{ m s}^{-1}$ not shown) and wind gust (m s^{-1} , shaded according to scale) on domain 4 valid at 0900 UTC 4 Jan 2009. The line from A to B shows the location of the cross section in Fig. 12.

Southington 2, Connecticut (G), observed significantly higher wind gusts than were forecast. However, these stations happen to be two of the three least forested in Table 2, suggesting that they were less sheltered from the wind than other locations.

A cross section taken parallel to the flow (and perpendicular to Kittatinny Mountain) shows the low-level jet more clearly than the model sounding (Fig. 12). Although subtle, a vertically propagating wave can be discerned above High Point by the slightly upshear-tilted depression in the isentropes. Much more readily seen is the trapped lee wave whose amplitude is maximized within the inversion. The wavelength of this lee wave (5.3 km) is much shorter than the wavelength of the topographic

forcing (the width of the ridge is about 20 km), and it is this disparity, along with the short distance between the ridgetop and inversion base, that allows for such strong nonlinear amplification to occur (Vosper 2004). The amplitude of the lee waves is not large enough to bring about wave breaking and a hydraulic jump, but it is large enough to generate a rotor (note the region of return flow in the lee of the ridge) and significant enhancement of the wind just to the lee of the ridge, matching the results of Vosper (2004). Bringing the high-momentum air down to the surface from approximately 925 hPa would account for most of the observed wind gusts. Although rotors are known as regions of extreme turbulence that can be hazardous to aviation (Hertenstein 2009), it appears that

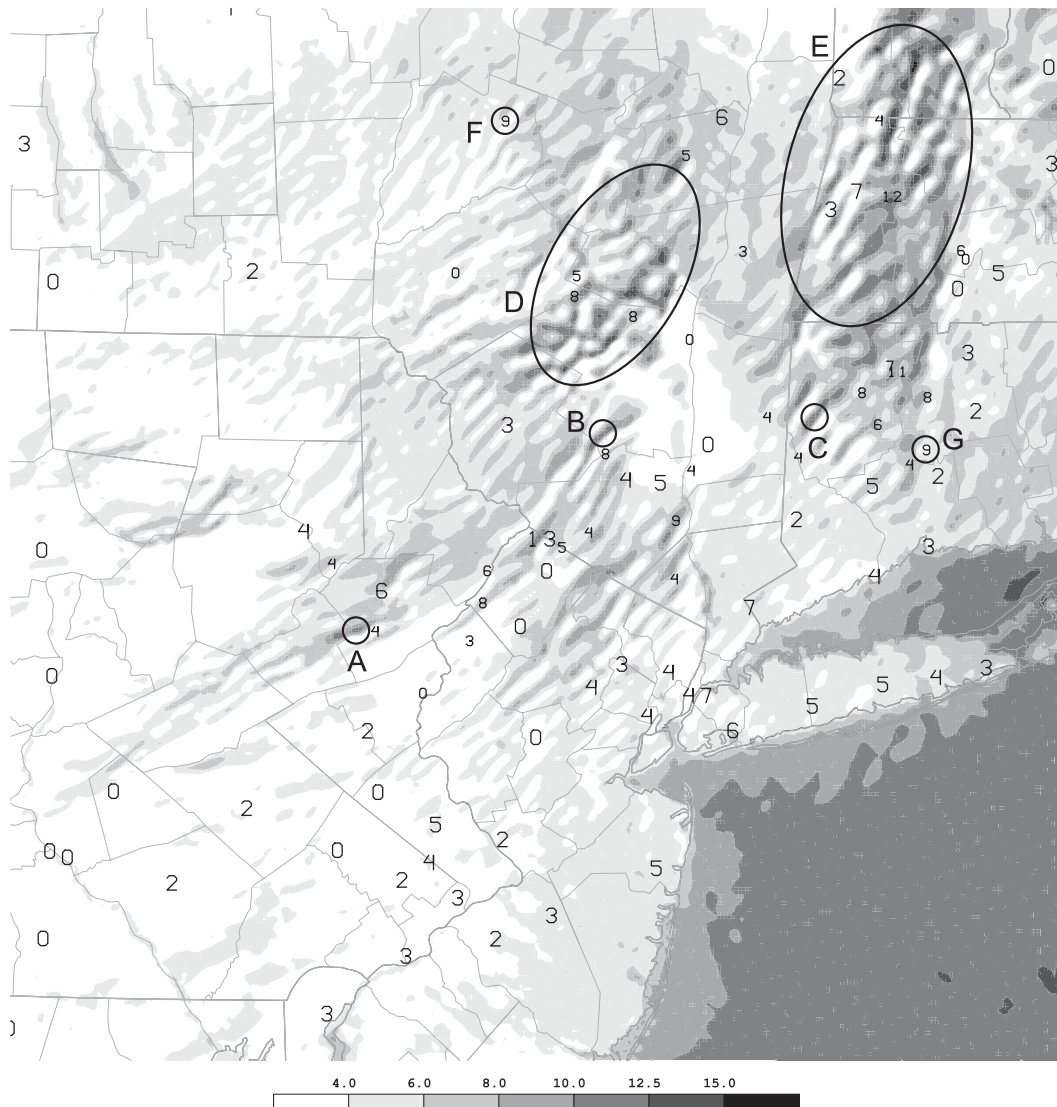


FIG. 11. The 9-h forecast of 10-m wind speed (m s^{-1} , shaded according to scale) valid at 0900 UTC 4 Jan 2009 on domain 4. Corresponding observed wind speeds (m s^{-1}) from ASOS stations and WNT (large text) and wind gusts (m s^{-1}) from the Mesowest network (small text) are also displayed. Labeled regions are discussed in the text.

High Point is removed just far enough from the busy New York City airports to eliminate significant risks to those aircraft. This is in contrast to the situation in the Falkland Islands analyzed by Sheridan and Vosper (2006), where turbulence associated with rotors frequently affects an airstrip in the immediate lee of local mountains.

What model resolution is necessary to capture the essence of this windstorm? Cairns and Corey (2003) found that 3-km grid spacing was necessary to simulate windstorms in Nevada, whereas Koletsis et al. (2009) suggested 2 km was necessary for their Greek windstorm. The terrain data from Fig. 7 hint that similar results would hold in this case, and Fig. 13 confirms this. Model wind and wind gust forecasts were compared with the

observations over the 16 h between 0100 and 1600 UTC, and the RMS error was computed for each station and wind type. For HPM, the instantaneous wind was compared to both the wind and wind gust forecasts. Although the poor siting of HPT confounds the errors at that station, the model captured the weak winds (but not the absence of wind gusts) at FWN across all domains. For the stations where the windstorm occurred, however, wind forecasts generally improved as resolution increased up to domain 4, with small changes thereafter. Table 4 shows a similar pattern in the model's ability to capture the peak sustained winds at WNT. The quickest increase in accuracy occurs between domains 2 and 4, but a portion of the high winds cannot be captured, even on

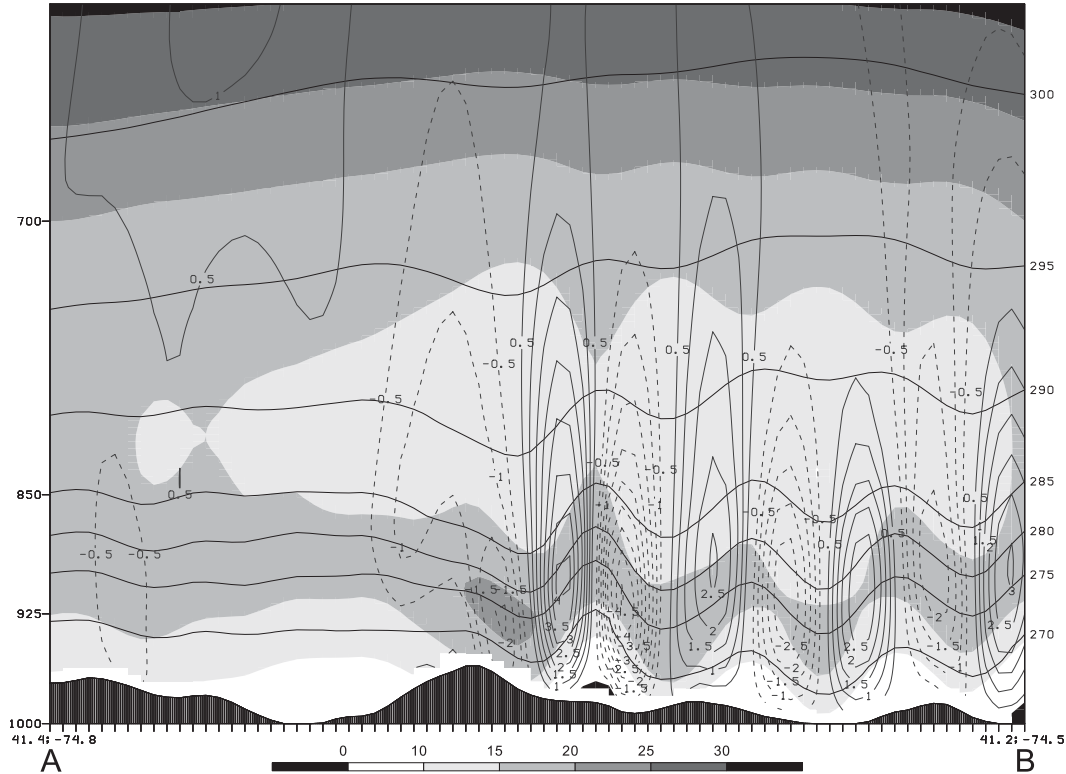


FIG. 12. Cross section parallel to the flow passing over High Point containing potential temperature (thick contours, every 5 K), vertical motion [thin contours, every 0.5 m s^{-1} , positive (negative) values solid (dashed) and zero line omitted], and wind component tangent to the cross section (m s^{-1} , shaded according to scale).

domain 5. Thus, while a grid spacing of around 1.33 km was adequate to capture the key elements of this event, some combination of forecast error in the atmospheric profile and inadequate terrain data prevents the full fury of the winds from being forecast. Needless to say, operational model output valid at this time (not shown) was not able to capture these winds, nor indicate any mountain wave signatures of the type used to forecast strong winds in portions of the West (Lindley et al. 2006).

To examine the predictability of the High Point windstorm, a second WRF forecast was produced, but with the model integration initialized at 0000 UTC 3 January 2009, 24 h earlier. To save computation time, inner nests were launched at 6-h intervals such that domain 5 began at 0000 UTC 4 January 2009. The resulting forecasts are most illuminating on domain 4, which is displayed in Fig. 14. Compare the original forecast of sustained lowest-model-level winds (Fig. 14a) with the same forecast derived from the earlier initialization time (Fig. 14b). In general, the strongest winds are less widespread in the earlier forecast, even over the open waters of the Atlantic Ocean, suggesting that the synoptic-scale winds were reduced in this earlier forecast. However, despite those weaker winds, the forecast

still shows a significant wind enhancement over and just to the lee of High Point. In addition, a few notable finescale structure differences exist. For instance, the earlier forecast emphasizes stronger winds north of High Point along the ridge into New York, whereas the later forecast centers strong winds on High Point itself. In fact, the ridge north of High Point is one of the few locations where the forecasted winds were stronger in the forecast based on the earlier initialization.

5. Concluding discussion

A localized and unanticipated downslope windstorm occurred in northern New Jersey during the early morning hours of 4 January 2009. Winds gusted to 30 m s^{-1} in a county where the forecast called for at most 5 m s^{-1} . Stations in the New Jersey Weather and Climate Network were well sited to observe the windstorm. Soundings in the region revealed that a strong temperature inversion was present that served as a waveguide along which lee waves could develop. Additional observations were sparse. Thus, a successful numerical model simulation was used to allow further analysis of the windstorm and estimation of its predictability. The simulation showed that nonlinear

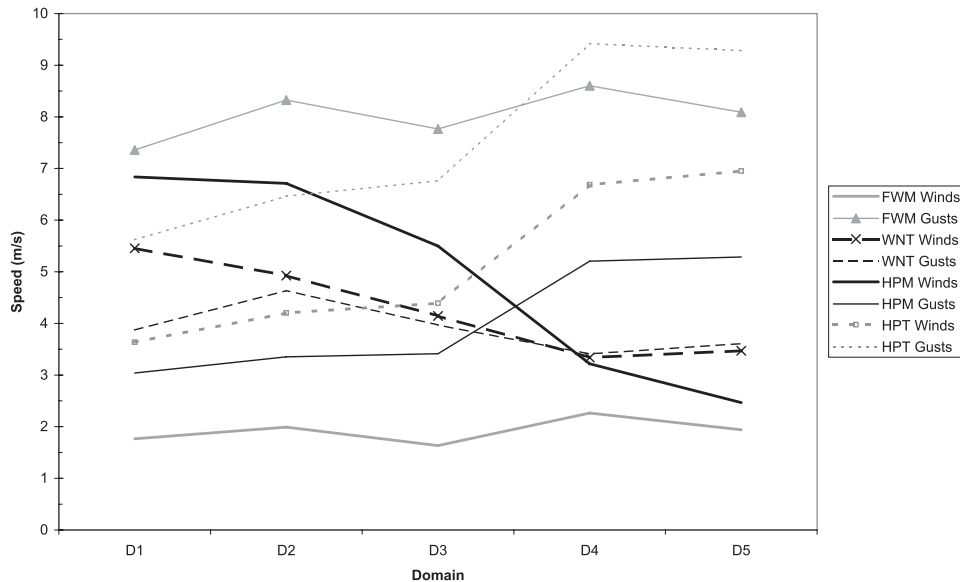


FIG. 13. The variation in the RMS error of wind and wind gust forecasts (m s^{-1}) with model domain. Shown are errors for WNT wind speed (thick, long-dashed line with cross) and gust (thin, medium-dashed line), HPM wind speed (thick, solid line) and gust (thin, solid line), HPT wind speed (thick, short-dashed line with square) and gust (thin, short-dashed line), and FWN wind speed (thick, solid gray line) and gust (thin, solid gray line with triangles).

interactions greatly enhanced the near-surface winds in accordance with the results of Vosper (2004). In particular, trapped lee waves with rotors were likely present, if not a hydraulic jump.

Since there was no clear sign of wave breaking, the use of the phrase “downslope windstorm” may be debatable. On the other hand, Durran (1986) suggests that windstorms do not require wave breaking, and Reinecke and Durran (2009a) refer to a “severe downslope windstorm with winds exceeding 25 m s^{-1} ,” which would also describe the event of 4 January 2009. At the very least, it is reasonable to conclude that mountain waves were involved in producing the strong, gusty winds that were observed.

Some of the features peculiar to this wind event were the presence of a northwesterly low-level jet within an extreme temperature inversion. However, similar features have been observed in Norway (Doyle and Shapiro 2000) and the Great Smoky Mountains (Gaffin 2002, 2009). In those cases, a southerly low-level jet impinged upon east–west-oriented mountains, and an inversion associated with an approaching warm front provided the mechanism for trapping the waves, but these frontal inversions were not as strong as the High Point inversion, and a critical level was often present. The conditions associated with windstorms in the central Appalachians (Manuel and Keighton 2010) are also reminiscent of this event, although the inversion is somewhat weaker and the winds are somewhat stronger in those cases.

Windstorms of this type present significant forecast challenges given the extremely small spatial scales involved. On the one hand, given the remote area, whether the winds could be forecast accurately may seem to be of academic interest. On the other hand, the small scale of the National Digital Forecast Database (Glahn and Ruth 2003), which includes wind gust forecasts, suggests that such small features cannot be ignored. Even with a high-resolution numerical model, forecasting these events is challenged by the propensity for models to overpredict windstorms (Nance and Coleman 2000) and the notable sensitivity to initial conditions that have been documented (Reinecke and Durran 2009a), which leads to uncertain forecasts even 12 h in advance.

It appears that this windstorm was localized to High Point. While observations confirmed this farther south along Kittatinny Mountain, no observations were available to the north, where model forecasts suggest strong winds

TABLE 4. Maximum 10-m wind speeds at WNT between 0100 and 1600 UTC 4 Jan 2009 from the various WRF domains and observations.

Source	Max speed (m s^{-1})
Domain 1	4.86
Domain 2	5.78
Domain 3	9.02
Domain 4	11.71
Domain 5	12.48
Observations	15.2

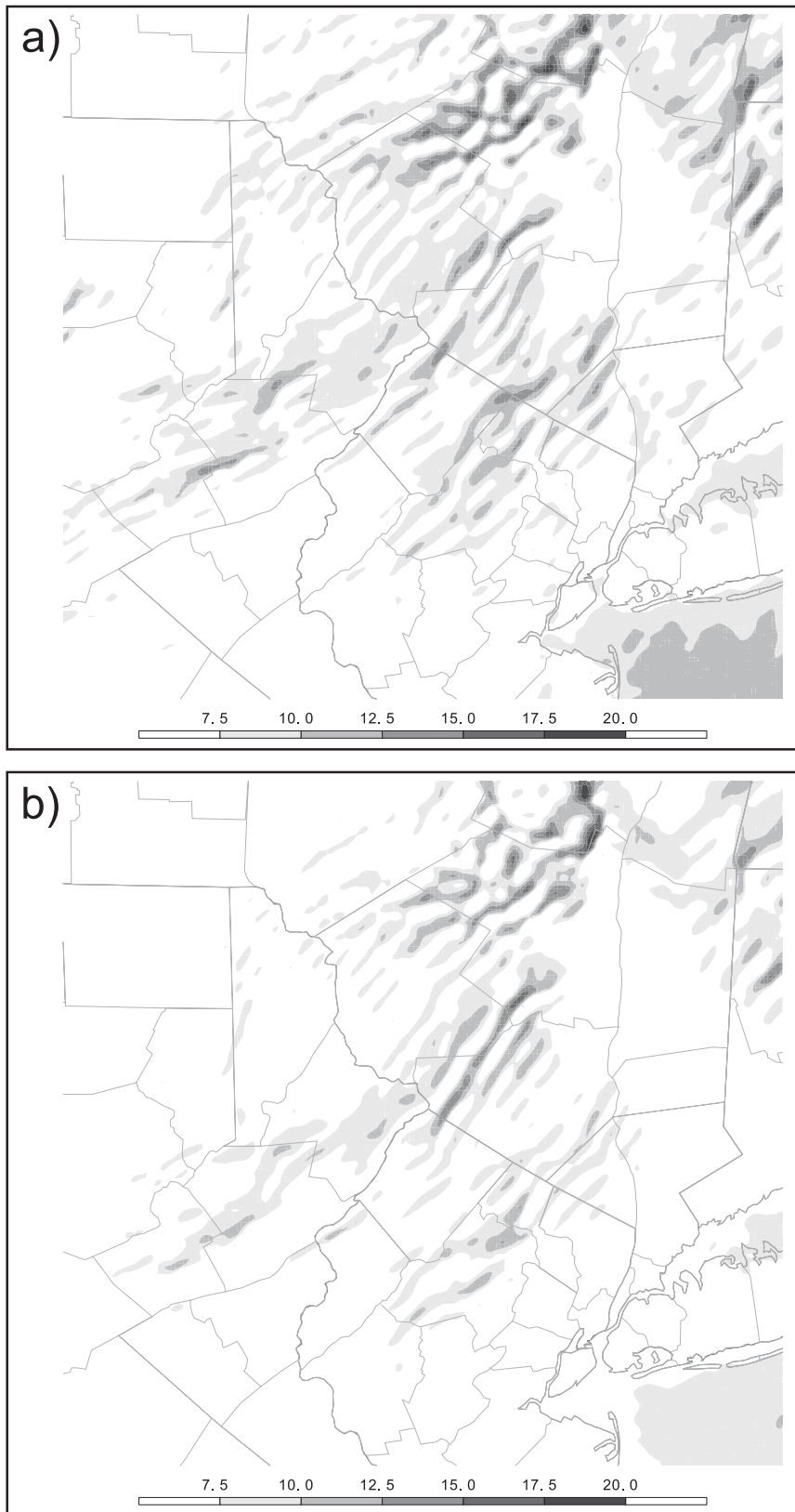


FIG. 14. WRF forecasts of sustained wind (m s^{-1} , shaded according to scale) on the lowest model level valid at 0900 UTC 4 Jan 2009 on domain 4. The forecasts are initialized at (a) 0000 UTC 4 Jan and (b) 0000 UTC 3 Jan 2009.

may also have occurred (B in Fig. 11). Should new surface observations of high winds elsewhere in the Northeast become available, forecasters can use the results of this study to guide their investigations.

Downslope windstorms near High Point appear to be infrequent. It may be that the inversion height must be in a very narrow range to produce the wind enhancement that was observed, as suggested by Klemp and Lilly (1975), thus leading to the rarity of this type of event. A preliminary investigation of wind measurements from HPM, WNT, and FWN over the three cold seasons between 2007 and 2010 suggests that about three events occur each year where strong winds at or near High Point and weak winds at FWN are simultaneously present. In agreement with the results of Jiang and Doyle (2008), all but one of these events occurred during nighttime hours. However, the case discussed herein is the only windstorm in which winds at FWN never gusted above 8 m s^{-1} . Therefore, the other events identified above likely do not reflect the 75% wind amplification that occurred during this case. In other words, winds may have been stronger at all levels over a broader area in at least some of the other cases. Further research is planned to address more adequately the climatology of these events.

Acknowledgments. The research described here was funded in part by the New Jersey Agricultural Experiment Station. Nick Stefano, Mathieu Gerbush, and Jacob Carlin obtained and helped analyze the surface observations, which were provided by the New Jersey Weather and Climate Network (a collection of surface weather stations administered by the Office of the New Jersey State Climatologist) and Mesowest. Three anonymous reviewers helped clarify this work.

REFERENCES

- Bosart, L. F., A. Seimon, K. D. LaPenta, and M. J. Dickinson, 2006: Supercell tornadogenesis over complex terrain: The Great Barrington, Massachusetts, tornado on 29 May 1995. *Wea. Forecasting*, **21**, 897–922.
- Brady, R. H., and J. S. Waldstreicher, 2001: Observations of mountain wave–induced precipitation shadows over northeast Pennsylvania. *Wea. Forecasting*, **16**, 281–300.
- Cairns, M. M., and J. Corey, 2003: Mesoscale model simulations of high-wind events in the complex terrain of western Nevada. *Wea. Forecasting*, **18**, 249–263.
- Chen, F., and J. Dudhia, 2001: Coupling an advanced land surface–hydrology model with the Penn State–NCAR MM5 modeling system. Part I: Model implementation and sensitivity. *Mon. Wea. Rev.*, **129**, 569–585.
- Chuang, H.-Y., G. DiMego, M. Baldwin, and WRF DTC Team, 2004: NCEP’s WRF post processor and verification systems. Preprints, *Fifth WRF/14th MM5 Users’ Workshop*, Boulder, CO, NCAR. [Available online at <http://www.mmm.ucar.edu/mm5/workshop/ws04/Session7/Chuang,Hui-Ya.pdf>].
- Clark, T. L., and W. R. Peltier, 1984: Critical level reflection and the resonant growth of nonlinear mountain waves. *J. Atmos. Sci.*, **41**, 3122–3134.
- Colle, B. A., and C. F. Mass, 1998a: Windstorms along the western side of the Washington Cascade Mountains. Part I: A high-resolution observational and modeling study of the 12 February 1995 event. *Mon. Wea. Rev.*, **126**, 28–52.
- , and —, 1998b: Windstorms along the western side of the Washington Cascade Mountains. Part II: Characteristics of past events and three-dimensional idealized simulations. *Mon. Wea. Rev.*, **126**, 53–71.
- Doyle, J. D., and M. A. Shapiro, 2000: A multi-scale simulation of an extreme downslope windstorm over complex topography. *Meteor. Atmos. Phys.*, **74**, 83–101.
- , and D. R. Durran, 2002: The dynamics of mountain-wave-induced rotors. *J. Atmos. Sci.*, **59**, 186–201.
- Dudhia, J., 1989: Numerical study of convection observed during the Winter Monsoon Experiment using a mesoscale two-dimensional model. *J. Atmos. Sci.*, **46**, 3077–3107.
- Durran, D. R., 1986: Another look at downslope windstorms. Part I: On the development of analogs to supercritical flow in an infinitely deep continuously stratified fluid. *J. Atmos. Sci.*, **43**, 2527–2543.
- , and J. B. Klemp, 1983: A compressible model for the simulation of moist mountain waves. *Mon. Wea. Rev.*, **111**, 2341–2361.
- Epifanio, C. C., and D. R. Durran, 2001: Three-dimensional effects in high-drag-state flows over long ridges. *J. Atmos. Sci.*, **58**, 1051–1065.
- Gaffin, D. M., 2002: Unexpected warming induced by foehn winds in the lee of the Smoky Mountains. *Wea. Forecasting*, **17**, 907–915.
- , 2009: On high winds and foehn warming associated with mountain-wave events in the western foothills of the southern Appalachian Mountains. *Wea. Forecasting*, **24**, 53–75.
- Glahn, H. R., and D. P. Ruth, 2003: The new digital forecast database of the National Weather Service. *Bull. Amer. Meteor. Soc.*, **84**, 195–201.
- Grisogono, B., and D. Belusic, 2009: A review of recent advances in understanding the meso- and microscale properties of the severe bora wind. *Tellus*, **61A**, 1–16.
- Hertenstein, R. F., 2009: The influence of inversions on rotors. *Mon. Wea. Rev.*, **137**, 433–446.
- Hildebrandt, M., and R. Balling, 1998: Climate variability at the world’s windiest weather station. *Windswept: Quart. Bull. Mt. Washington Obs.*, **39**, 34–40.
- Hong, S.-Y., and J.-O. Lim, 2006: The WRF single-moment 6-class microphysics scheme (WSM6). *J. Korean Meteor. Soc.*, **42**, 129–151.
- , Y. Noh, and J. Dudhia, 2006: A new vertical diffusion package with an explicit treatment of entrainment processes. *Mon. Wea. Rev.*, **134**, 2318–2341.
- Horel, J., and Coauthors, 2002: Mesowest: Cooperative mesonets in the western United States. *Bull. Amer. Meteor. Soc.*, **83**, 211–226.
- Jiang, Q., and J. D. Doyle, 2008: On the diurnal variation of mountain waves. *J. Atmos. Sci.*, **65**, 1360–1377.
- Kain, J. S., 2004: The Kain–Fritsch convective parameterization: An update. *J. Appl. Meteor.*, **43**, 170–181.
- Klemp, J. B., and D. K. Lilly, 1975: The dynamics of wave-induced downslope winds. *J. Atmos. Sci.*, **32**, 320–339.
- Koletsis, I., K. Lagouvardos, V. Kotroni, and A. Bartzokas, 2009: Numerical study of a downslope windstorm in northwestern Greece. *Atmos. Res.*, **94**, 178–193.
- Lindley, T. T., C. Lindsey, and J. Cupo, 2006: An operational technique used to detect “mountain wave signatures”: A

- forecast methodology for severe westerly winds in the mountains of west Texas. Preprints, *12th Conf. on Mesoscale Processes*, Santa Fe, NM, Amer. Meteor. Soc., 15.4. [Available online at <http://ams.confex.com/ams/pdfpapers/110055.pdf>.]
- Manuel, P., and S. Keighton, cited 2010: Anticipating damaging foehn windstorms east of the central Appalachians. [Available online at <http://ams.confex.com/ams/pdfpapers/62410.pdf>.]
- Martner, B. E., R. F. Reinking, and R. M. Banta, 2002: Radar observations of downslope flow at Mount Washington. Preprints, *10th Conf. on Mountain Meteorology*, Park City, UT, Amer. Meteor. Soc., 16.4. [Available online at <http://ams.confex.com/ams/pdfpapers/39778.pdf>.]
- Meyers, M. P., J. S. Snook, D. A. Wesley, and G. S. Poulos, 2003: A Rocky Mountain storm. Part II: The forest blowdown over the west slope of the northern Colorado mountains—Observations, analysis, and modeling. *Wea. Forecasting*, **18**, 662–674.
- Miller, P. P., and D. R. Durran, 1991: On the sensitivity of downslope windstorms to the asymmetry of the mountain profile. *J. Atmos. Sci.*, **48**, 1457–1473.
- Mlawer, E. J., S. J. Taubman, P. D. Brown, M. J. Iacono, and S. A. Clough, 1997: Radiative transfer for inhomogeneous atmosphere: RRTM, a validated correlated-k model for the longwave. *J. Geophys. Res.*, **102** (D14), 16 663–16 682.
- Monin, A. S., and A. M. Obukhov, 1954: Basic laws of turbulent mixing in the surface layer of the atmosphere (in Russian). *Contrib. Geophys. Inst. Acad. Sci., USSR*, **151**, 163–187.
- Nance, L. B., and B. R. Coleman, 2000: Evaluating the use of a nonlinear two-dimensional model in downslope windstorm forecasts. *Wea. Forecasting*, **15**, 715–729.
- Reinecke, P. A., and D. R. Durran, 2009a: Initial-condition sensitivities and the predictability of downslope winds. *J. Atmos. Sci.*, **66**, 3401–3418.
- , and —, 2009b: The overamplification of gravity waves in numerical solutions to flow over topography. *Mon. Wea. Rev.*, **137**, 1533–1549.
- Robinson, D. A., 2005: The New Jersey Weather and Climate Network: Providing environmental information for a myriad of applications. Preprints, *15th Conf. on Applied Climatology*, Savannah, GA, Amer. Meteor. Soc., J2.1. [Available online at <http://ams.confex.com/ams/pdfpapers/94206.pdf>.]
- Sheridan, P. F., and S. B. Vosper, 2006: A flow regime diagram for forecasting lee waves, rotors, and downslope winds. *Meteor. Appl.*, **13**, 179–195.
- Skamarock, W. C., and Coauthors, 2008: A description of the Advanced Research WRF version 3. NCAR Tech. Note NCAR/TN-475+STR, 113 pp.
- Thompson, R. L., R. Edwards, J. A. Hart, K. L. Elmore, and P. Markowski, 2003: Close proximity soundings within supercell environments obtained from the Rapid Update Cycle. *Wea. Forecasting*, **18**, 1243–1261.
- Vosper, S. B., 2004: Inversion effects on mountain lee waves. *Quart. J. Roy. Meteor. Soc.*, **130**, 1723–1748.